COLD CONDITIONS PROMOTE MG AND SI INCORPORATION IN FE/SI-RICH AND AL-POOR X-RAY AMORPHOUS MATERIAL IN MARS-RELEVANT FIELD ENVIRONMENTS.

A.D. Feldman[1,2], E.M. Hausrath[1], E.B. Rampe[3], T. Sharp[4], O. Tschauner[1], M. Newville[5], A. Lanzirotti[5]. [1]Univ. of Nevada Las Vegas, Las Vegas NV, [2]Now at Desert Research Institute, Las Vegas, NV (anthony.feldman@dri.edu), [3]Johnson Space Center, Houston TX, [4]Arizona State Univ., Tempe AZ, [5]University of Chicago, Chicago IL

Introduction: X-ray amorphous material that is variably Fe/Si-rich, Al-poor, and volatile containing is prevalent (~15-73 wt.%) within ancient fluvial-lacustrine and eolian sediments examined by the CheMin instrument in Gale crater [1, 2]. Al-rich X-ray amorphous material within Mars-analog environments [3,4] on Earth has previously been proposed to result from aqueous alteration under cold and icy conditions [4]. However, to the best of our knowledge, no work to date has examined the effects of climate upon the formation of Al-poor and Fe/Si-rich X-ray amorphous material. This study therefore investigates the production of Al-poor and Fe-containing X-ray amorphous material and the chemical heterogeneity within that material under varying temperature conditions to better interpret the formation of Fe-containing X-ray amorphous material detected on Mars.

Methods:

Field Sites We examined two ultramafic soils from the Mediterranean climate Klamath Mountains (KM) of California termed Eunice Bluff (EB) and String Bean Creek (SBC) and two from the subarctic climate Tablelands (TB) of Newfoundland, Canada termed Devil's Punchbowl (DvP) and Trout River Gulch (TRG). KM sites experience mean temperatures of ~12.8°C and precipitation of ~101-118 cm/year [5,6], high-elevation regions in the KM such as EB (~2100 m) experience extended periods of far-below-freezing conditions [7] not found at the lower elevation (~1000 m) SBC site [5,6]. TB sites experience mean temperatures of ~3.9°C and precipitation of ~120 cm/year [8].

Soil Sampling and Preparation Soil pits were hand excavated and samples collected from the visually most weathered soil horizon. Samples were sieved to separate bulk soil (<2 mm diameter) from gravel followed by extraction of the clay-size fraction (<2 µm diameter) by sonication and settling [9]. Bulk soil material was shipped to Wagner Petrographic Inc. for preparation of thin-section grain mounts polished to a 0.25-micron level using mineral spirits.

Analytical Techniques Clay-size fraction material was analyzed on lacey-carbon Cu grids on a Titan 300/80 (FEI) TEM at 300 kV at ASU to investigate chemical heterogeneity within X-ray amorphous material. Bulk soil grain mounts were analyzed by µXRD at the Argonne National Laboratory beamline 13-ID-E (0.6888Å wavelength). Phase ID in µXRD was determined through Rietveld refinement in Profex [10] using crystallographic information files from the Crystallography Open Database [11].

Results and Discussion: X-ray amorphous material in these soils includes globular amorphous silica (Figure 1) and a "clumpy" [12] mixed-oxide amorphous material that is morphologically like the clumpy/fluffy X-ray amorphous material of [3,4]. The globular amorphous silica appears as isolated aggregates (Figure 1), consistent with precipitation from solution. The clumpy material is composed of an amorphous aggregate of nanospherules and a nanocrystallite component (Figure 2). Clumpy X-ray amorphous material was observed coating agglomerations of crystalline material and as isolated aggregates (Figure 2), consistent with formation through dissolution/precipitation reactions and potentially through precipitation from solution. Glasses indicative of primary amorphous material were not observed.
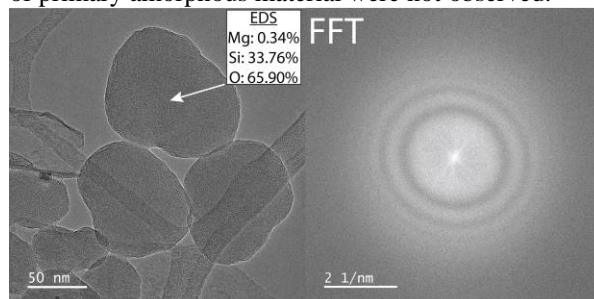

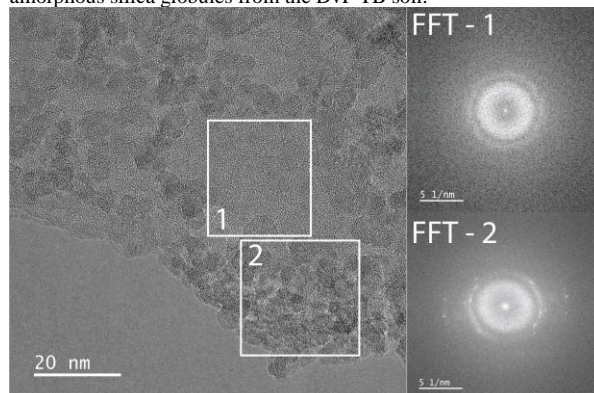Figure 1: TEM and Fast Fourier transform (FFT) images of amorphous silica globules from the DvP TB soil.

Figure 2: TEM and FFT images of mixed nanospherical amorphous material (1) and nanocrystallites (2) from the EB KM soil

The chemical makeup of clumpy material exhibits a robust correlation with temperature. Clumpy material is Al-poor (≤4.7 atom %), sometimes Mg-containing (0-18.15 atom %), and is variably rich in Fe (4.29-39.86

atom %) and Si (0-39.01 atom %), chemically like Gale crater X-ray amorphous material [1,2]. Clumpy material in TB soils is on average richer in Mg and Si than in the KM soils (Figure 3). This chemical trend is particularly pronounced for nanocrystallite containing clumpy material (Figure 3), for which KM nanocrystallites are almost entirely Fe-containing (mean Fe: 30.62 atom %) while TB nanocrystallites contain roughly equal amounts of mean Mg + Si (21.58 atom %) and Fe (20.83 atom %).
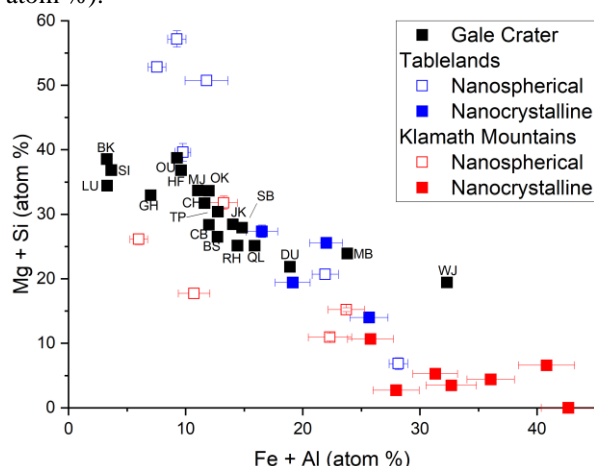

Figure 3: Relatively mobile Mg+Si vs immobile Fe+Al element concentrations in terrestrial X-ray amorphous material compared to Gale crater ancient fluvial and aeolian sediment X-ray amorphous material. Gale crater abbreviations and concentrations are from [1].

The Fe-rich nature of the nanocrystallites is likely due to growth of Fe^{3+}-oxyhydroxide nanominerals. While nanocrystallite d-spacings extracted from FFT images do not exactly match known mineral phases, at least two lattice planes consistent with goethite were observed in FFTs from all examined nanocrystallite-containing areas. Goethite is present in µXRD patterns of weathering rinds (Figure 4), consistent with formation of goethite nanoparticles within X-ray amorphous material. Elevated Mg+Si in TB compared with KM nanocrystallites is consistent with limited goethite nanocrystallite formation under colder temperatures within a Mg/Si-rich nanospherical matrix, consistent with the greater abundance of goethite within KM weathering rinds measured by µXRD (Figure 4).

The presence of globular amorphous silica correlates with extended sub-freezing temperature conditions. Amorphous silica was observed in both examined TB soils. However, in the KM soils, globular amorphous silica was only observed in the high-altitude (~2100 m) EB soil that undergoes extended periods of sub-freezing winter conditions but was not observed in the lower altitude (~1000 m) SBC soil that possesses average winter low temperatures that hover around freezing [5,6]. These results are consistent with colder temperatures lowering amorphous silica solubility [13], raising Si concentration in solution above amorphous SiO_2 saturation through freezing of soil-pore water during periods of extended sub-freezing temperature conditions.
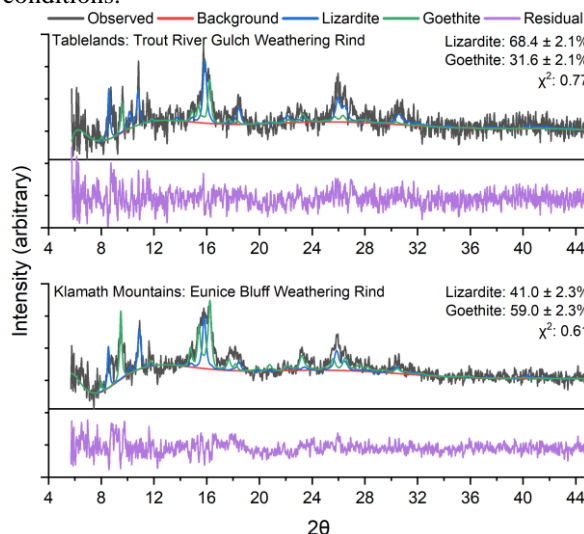

Figure 4: Rietveld fits (values in mass %) indicating goethite and lizardite within µXRD patterns from weathering rinds in the TRG soil in the TB (Top) and the EB soil in the KM (Bottom).

Martian Implications: Within these ultramafic soils, colder temperatures correlate with the presence of amorphous silica and greater retention of Mg and Si within Fe-containing X-ray amorphous material. Retention of Mg and Si under colder conditions is particularly pronounced for nanocrystallite-containing X-ray amorphous material. These results suggest the abundant Fe/Si-rich but generally more Si-rich than Fe-rich X-ray amorphous material in Gale crater [1,2] is consistent with formation under cold and icy conditions. Highly variable Mg content within Gale crater X-ray amorphous material [1] might reflect local variations in the non-ultramafic parent material Mg-content or variable smectite Mg content not captured in mass balance calculations. Microscale techniques such as TEM and synchrotron microprobe will likely prove valuable for evaluating the presence and nature X-ray amorphous material within returned Martian samples.

References: [1] Rampe et al. (2020) *Geochem.*, 80, 2, 125605. [2] Smith et al. (2018) *JGR* 123, 2485-2505 [3] Smith and Horgan (2021) *JGR*. 126, 5 [4] Rampe et al. (2022) *EPSL*. 584, 117471 [5] NOAA 1991-2020 Climate Normals [6] Skinner et al. (2006) *Univ. Cal Press* 170-194 [7] Garwood and Welsh (2007) Ecology of the Cascades frog... [8] Env. Can. 1981-2010 Climate Normals [9] Edwards and Bremner (1968) *J. Soil Sci.*, *18*(1), 64-73 [10] Doebelin and Kleeberg (2015) *J App. Cry.* 48, 5, 1573-1580 [11] Gražulis et al (2009) *J App. Cry* 42, 4, 726-729 [12] Ralston et al. (2021) *CCM* 69, 2, 263-288 [13] Gunnarsson and Arnórsson (2000) *GCA 64*, 13, 2295-2307